DESY 97-228 ISSN 0418-9833

Photo-production of $\psi(2S)$ Mesons at HERA

H1 Collaboration

Abstract

Quasi-elastic (z>0.95) photo-production of $\psi(2S)$ mesons has been observed at HERA for photon-proton centre-of-mass energies in the range 40 to 160 GeV. The $\psi(2S)$ mesons were identified through their decays to $\ell^+\ell^-$ and to $J/\psi \, \pi^+\pi^-$, where the J/ψ subsequently decays to $\ell^+\ell^-$, the lepton ℓ being either a muon or an electron. The cross-section for quasi-elastic photoproduction was measured to be $(18.0\pm2.8(\mathrm{stat})\pm3.0(\mathrm{syst}))$ nb at a photon-proton centre-of-mass energy of 80 GeV. The ratio of the $\psi(2S)$ to J/ψ quasi-elastic cross-sections is $(0.150\pm0.027(\mathrm{stat})\pm0.022(\mathrm{syst}))$.

Submitted to Physics Letters B

C. Adloff³⁵, S. Aid¹³, M. Anderson²³, V. Andreev²⁶, B. Andrieu²⁹, V. Arkadov³⁶, C. Arndt¹¹, I. Ayyaz³⁰, A. Babaev²⁵, J. Bähr³⁶, J. Bán¹⁸, P. Baranov²⁶, E. Barrelet³⁰, R. Barschke¹¹ W. Bartel¹¹, U. Bassler³⁰, M. Beck¹⁴, H.-J. Behrend¹¹, C. Beier¹⁶, A. Belousov²⁶, Ch. Berger¹ G. Bernardi³⁰, G. Bertrand-Coremans⁴, R. Beyer¹¹, P. Biddulph²³, J.C. Bizot²⁸, K. Borras⁸ V. Boudry²⁹, S. Bourov²⁵, A. Braemer¹⁵, W. Braunschweig¹, V. Brisson²⁸, D.P. Brown²³ W. Brückner¹⁴, P. Bruel²⁹, D. Bruncko¹⁸, C. Brune¹⁶, J. Bürger¹¹, F.W. Büsser¹³, A. Buniatian⁴, S. Burke¹⁹, G. Buschhorn²⁷, D. Calvet²⁴, A.J. Campbell¹¹, T. Carli²⁷, M. Charlet¹¹, D. Clarke⁵. B. Clerbaux⁴, S. Cocks²⁰, J.G. Contreras⁸, C. Cormack²⁰, J.A. Coughlan⁵, M.-C. Cousinou²⁴ B.E. Cox²³, G. Cozzika⁹, D.G. Cussans⁵, J. Cvach³¹, S. Dagoret³⁰, J.B. Dainton²⁰, W.D. Dau¹⁷, K. Daum⁴⁰, M. David⁹, A. De Roeck¹¹, E.A. De Wolf⁴, B. Delcourt²⁸, M. Dirkmann⁸, P. Dixon¹⁹ W. Dlugosz⁷, K.T. Donovan²¹, J.D. Dowell³, A. Droutskoi²⁵, J. Ebert³⁵, T.R. Ebert²⁰. G. Eckerlin¹¹, V. Efremenko²⁵, S. Egli³⁸, R. Eichler³⁷, F. Eisele¹⁵, E. Eisenhandler²¹, E. Elsen¹¹. M. Erdmann¹⁵, A.B. Fahr¹³, L. Favart²⁸, A. Fedotov²⁵, R. Felst¹¹, J. Feltesse⁹, J. Ferencei¹⁸ F. Ferrarotto³³, K. Flamm¹¹, M. Fleischer⁸, M. Flieser²⁷, G. Flügge², A. Fomenko²⁶ J. Formánek³², J.M. Foster²³, G. Franke¹¹, E. Gabathuler²⁰, K. Gabathuler³⁴, F. Gaede²⁷ J. Garvey³, J. Gayler¹¹, M. Gebauer³⁶, R. Gerhards¹¹, A. Glazov³⁶, L. Goerlich⁶, N. Gogitidze²⁶ M. Goldberg³⁰, B. Gonzalez-Pineiro³⁰, I. Gorelov²⁵, C. Grab³⁷, H. Grässler², T. Greenshaw²⁰ R.K. Griffiths²¹, G. Grindhammer²⁷, A. Gruber²⁷, C. Gruber¹⁷, T. Hadig¹, D. Haidt¹¹. L. Hajduk⁶, T. Haller¹⁴, M. Hampel¹, W.J. Haynes⁵, B. Heinemann¹¹, G. Heinzelmann¹³ R.C.W. Henderson¹⁹, S. Hengstmann³⁸, H. Henschel³⁶, R. Heremans⁴, I. Herynek³¹, K. Hewitt³. K.H. Hiller³⁶, C.D. Hilton²³, J. Hladký³¹, M. Höppner⁸, D. Hoffmann¹¹, T. Holtom²⁰ R. Horisberger³⁴, V.L. Hudgson³, M. Hütte⁸, M. Ibbotson²³, Ç. İşsever⁸, H. Itterbeck¹ M. Jacquet²⁸, M. Jaffre²⁸, J. Janoth¹⁶, D.M. Jansen¹⁴, L. Jönsson²², D.P. Johnson⁴, H. Jung²² P.I.P. Kalmus²¹, M. Kander¹¹, D. Kant²¹, U. Kathage¹⁷, J. Katzy¹⁵, H.H. Kaufmann³⁶, O. Kaufmann¹⁵, M. Kausch¹¹, S. Kazarian¹¹, I.R. Kenyon³, S. Kermiche²⁴, C. Keuker¹ C. Kiesling²⁷, M. Klein³⁶, C. Kleinwort¹¹, G. Knies¹¹, J.H. Köhne²⁷, H. Kolanoski³⁹ S.D. Kolya²³, V. Korbel¹¹, P. Kostka³⁶, S.K. Kotelnikov²⁶, T. Krämerkämper⁸, M.W. Krasny^{6,30} H. Krehbiel¹¹, D. Krücker²⁷, A. Küpper³⁵, H. Küster²², M. Kuhlen²⁷, T. Kurča³⁶, B. Laforge⁹, R. Lahmann¹¹, M.P.J. Landon²¹, W. Lange³⁶, U. Langenegger³⁷, A. Lebedev²⁶, F. Lehner¹¹ V. Lemaitre¹¹, S. Levonian²⁹, M. Lindstroem²², J. Lipinski¹¹, B. List¹¹, G. Lobo²⁸, G.C. Lopez¹². V. Lubimov²⁵, D. Lüke^{8,11}, L. Lytkin¹⁴, N. Magnussen³⁵, H. Mahlke-Krüger¹¹, E. Malinovski²⁶ R. Maraček¹⁸, P. Marage⁴, J. Marks¹⁵, R. Marshall²³, J. Martens³⁵, G. Martin¹³, R. Martin²⁰, H.-U. Martyn¹, J. Martyniak⁶, S.J. Maxfield²⁰, S.J. McMahon²⁰, A. Mehta⁵, K. Meier¹⁶ P. Merkel¹¹, F. Metlica¹⁴, A. Meyer¹³, A. Meyer¹¹, H. Meyer³⁵, J. Meyer¹¹, P.-O. Meyer², A. Migliori²⁹, S. Mikocki⁶, D. Milstead²⁰, J. Moeck²⁷, F. Moreau²⁹, J.V. Morris⁵, E. Mroczko⁶ D. Müller³⁸, K. Müller¹¹, P. Murín¹⁸, V. Nagovizin²⁵, R. Nahnhauer³⁶, B. Naroska¹³ Th. Naumann³⁶, I. Négri²⁴, P.R. Newman³, D. Newton¹⁹, H.K. Nguyen³⁰, T.C. Nicholls³ F. Niebergall¹³, C. Niebuhr¹¹, Ch. Niedzballa¹, H. Niggli³⁷, G. Nowak⁶, T. Nunnemann¹⁴ H. Oberlack²⁷, J.E. Olsson¹¹, D. Ozerov²⁵, P. Palmen², E. Panaro¹¹, A. Panitch⁴, C. Pascaud²⁸. S. Passaggio³⁷, G.D. Patel²⁰, H. Pawletta², E. Peppel³⁶, E. Perez⁹, J.P. Phillips²⁰, A. Pieuchot²⁴ D. Pitzl³⁷, R. Pöschl⁸, G. Pope⁷, B. Povh¹⁴, K. Rabbertz¹, P. Reimer³¹, H. Rick⁸, S. Riess¹³, E. Rizvi¹¹, P. Robmann³⁸, R. Roosen⁴, K. Rosenbauer¹, A. Rostovtsev³⁰ F. Rouse⁷, C. Royon⁹, K. Rüter²⁷, S. Rusakov²⁶, K. Rybicki⁶, D.P.C. Sankey⁵, P. Schacht²⁷ J. Scheins¹, S. Schiek¹¹, S. Schleif¹⁶, W. von Schlippe²¹, D. Schmidt³⁵, G. Schmidt¹¹ L. Schoeffel⁹, A. Schöning¹¹, V. Schröder¹¹, E. Schuhmann²⁷, H.-C. Schultz-Coulon¹¹ B. Schwab¹⁵, F. Sefkow³⁸, A. Semenov²⁵, V. Shekelyan¹¹, I. Sheviakov²⁶, L.N. Shtarkov²⁶ G. Siegmon¹⁷, U. Siewert¹⁷, Y. Sirois²⁹, I.O. Skillicorn¹⁰, T. Sloan¹⁹, P. Smirnov²⁶, M. Smith²⁰ V. Solochenko²⁵, Y. Soloviev²⁶, A. Specka²⁹, J. Spiekermann⁸, S. Spielman²⁹, H. Spitzer¹³, F. Squinabol²⁸, P. Steffen¹¹, R. Steinberg², J. Steinhart¹³, B. Stella³³, A. Stellberger¹⁶, J. Stiewe¹⁶, K. Stolze³⁶, U. Straumann¹⁵, W. Struczinski², J.P. Sutton³, M. Swart¹⁶ S. Tapprogge¹⁶, M. Taševský³², V. Tchernyshov²⁵, S. Tchetchelnitski²⁵, J. Theissen² G. Thompson²¹, P.D. Thompson³, N. Tobien¹¹, R. Todenhagen¹⁴, P. Truöl³⁸, G. Tsipolitis³⁷,

- J. Turnau 6, E. Tzamariudaki $^{11},$ P. Uelkes 2, A. Usik $^{26},$ S. Valkár $^{32},$ A. Valkárová $^{32},$ C. Vallée $^{24},$
- P. Van Esch⁴, P. Van Mechelen⁴, D. Vandenplas²⁹, Y. Vazdik²⁶, P. Verrecchia⁹, G. Villet⁹,
- K. Wacker⁸, A. Wagener², M. Wagener³⁴, R. Wallny¹⁵, T. Walter³⁸, B. Waugh²³, G. Weber¹³
- M. Weber¹⁶, D. Wegener⁸, A. Wegner²⁷, T. Wengler¹⁵, M. Werner¹⁵, L.R. West³, S. Wiesand³⁵
- T. Wilksen¹¹, S. Willard⁷, M. Winde³⁶, G.-G. Winter¹¹, C. Wittek¹³, M. Wobisch², H. Wollatz¹¹,
- E. Wünsch¹¹, J. Žáček³², J. Zálešák³², D. Zarbock¹², Z. Zhang²⁸, A. Zhokin²⁵, P. Zini³⁰,
- F. Zomer²⁸, J. Zsembery⁹, and M. zurNedden³⁸,
- $^{\rm 1}$ I. Physikalisches Institut der RWTH, Aachen, Germany $^{\rm a}$
- ² III. Physikalisches Institut der RWTH, Aachen, Germany^a
- 3 School of Physics and Space Research, University of Birmingham, Birmingham, UK^b
- 4 Inter-University Institute for High Energies ULB-VUB, Brussels; Universitaire Instelling Antwerpen, Wilrijk; Belgium^c
- 5 Rutherford Appleton Laboratory, Chilton, Didcot, \mathbf{UK}^{b}
- ⁶ Institute for Nuclear Physics, Cracow, Poland^d
- 7 Physics Department and IIRPA, University of California, Davis, California, USA e
- ⁸ Institut für Physik, Universität Dortmund, Dortmund, Germany^a
- ⁹ DSM/DAPNIA, CEA/Saclay, Gif-sur-Yvette, France
- ¹⁰ Department of Physics and Astronomy, University of Glasgow, Glasgow, UK^b
- ¹¹ DESY, Hamburg, Germany^a
- ¹² I. Institut für Experimentalphysik, Universität Hamburg, Hamburg, Germany^a
- ¹³ II. Institut für Experimentalphysik, Universität Hamburg, Hamburg, Germany^a
- ¹⁴ Max-Planck-Institut für Kernphysik, Heidelberg, Germany^a
- ¹⁵ Physikalisches Institut, Universität Heidelberg, Heidelberg, Germany^a
- ¹⁶ Institut für Hochenergiephysik, Universität Heidelberg, Heidelberg, Germany^a
- ¹⁷ Institut für Reine und Angewandte Kernphysik, Universität Kiel, Kiel, Germany^a
- 18 Institute of Experimental Physics, Slovak Academy of Sciences, Košice, Slovak Republic f,j
- ¹⁹ School of Physics and Chemistry, University of Lancaster, Lancaster, UK^b
- ²⁰ Department of Physics, University of Liverpool, Liverpool, UK^b
- ²¹ Queen Mary and Westfield College, London, UK^b
- ²² Physics Department, University of Lund, Lund, Sweden^g
- 23 Physics Department, University of Manchester, Manchester, UK^b
- ²⁴ CPPM, Université d'Aix-Marseille II, IN2P3-CNRS, Marseille, France
- ²⁵ Institute for Theoretical and Experimental Physics, Moscow, Russia
- ²⁶ Lebedev Physical Institute, Moscow, Russia^{f,k}
- ²⁷ Max-Planck-Institut für Physik, München, Germany^a
- ²⁸ LAL, Université de Paris-Sud, IN2P3-CNRS, Orsay, France
- ²⁹ LPNHE, Ecole Polytechnique, IN2P3-CNRS, Palaiseau, France
- ³⁰ LPNHE, Universités Paris VI and VII, IN2P3-CNRS, Paris, France
- ³¹ Institute of Physics, Czech Academy of Sciences of the Czech Republic, Praha, Czech Republic^{f,h}
- 32 Nuclear Center, Charles University, Praha, Czech Republic f,h
- ³³ INFN Roma 1 and Dipartimento di Fisica, Università Roma 3, Roma, Italy
- ³⁴ Paul Scherrer Institut, Villigen, Switzerland
- ³⁵ Fachbereich Physik, Bergische Universität Gesamthochschule Wuppertal, Wuppertal, Germany^a
- ³⁶ DESY, Institut für Hochenergiephysik, Zeuthen, Germany^a
- ³⁷ Institut für Teilchenphysik, ETH, Zürich, Switzerlandⁱ
- ³⁸ Physik-Institut der Universität Zürich, Zürich, Switzerlandⁱ
- 39 Institut für Physik, Humboldt-Universität, Berlin, Germany a
- ⁴⁰ Rechenzentrum, Bergische Universität Gesamthochschule Wuppertal, Wuppertal, Germany^a
- a Supported by the Bundesministerium für Bildung, Wissenschaft, Forschung und Technologie, FRG, under contract numbers 7AC17P, 7AC47P, 7DO55P, 7HH17I, 7HH27P, 7HD17P, 7HD27P, 7KI17I, 6MP17I and 7WT87P
- b Supported by the UK Particle Physics and Astronomy Research Council, and formerly by the UK Science and Engineering Research Council
- c Supported by FNRS-NFWO, IISN-IIKW
- d Partially supported by the Polish State Committee for Scientific Research, grant no. 115/E-343/SPUB/P03/002/97 and grant no. 2P03B 055 13

- e Supported in part by US DOE grant DE F603 91ER40674
- f Supported by the Deutsche Forschungsgemeinschaft
- g Supported by the Swedish Natural Science Research Council
- h Supported by GA ČR grant no. 202/96/0214, GA AV ČR grant no. A1010619 and GA UK grant no. 177
- i Supported by the Swiss National Science Foundation
- j Supported by VEGA SR grant no. 2/1325/96
- k Supported by Russian Foundation for Basic Researches grant no. 96-02-00019

1 Introduction

At HERA the production of vector mesons is studied at photon-proton centre-of-mass energies $(W_{\gamma p})$ extending well beyond those reached in fixed target experiments. In particular, the production of J/ψ mesons has been reported upon by H1 [1, 2, 3] and ZEUS [4, 5, 6]. In this letter a study of the quasi-elastic photo-production of $\psi(2S)$, i.e. $\psi(3685)$, mesons in the photon-proton centre-of-mass energy range $40 < W_{\gamma p} < 160$ GeV is reported. Quasi-elastic is defined here as the kinematic region z > 0.95, where $z = E_{\psi(2S)}/E_{\gamma}$ in the rest frame of the proton. The $\psi(2S)$ mesons are identified via the decays $\psi(2S) \to J/\psi(\to \ell^+\ell^-)\pi^+\pi^-$ or $\psi(2S) \to \ell^+\ell^-$, where ℓ denotes a muon or an electron.

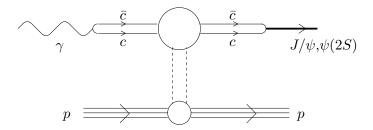


Figure 1: Elastic production of charmonium

At the collision energies studied here, the process $\gamma p \to V p$ $(V=J/\psi \text{ or } \psi(2S))$ can be considered in three parts (see figure 1): the formation of a $c\bar{c}$ quark pair from the photon, the interaction of the quark pair with the proton, and subsequently the formation of the charmonium state. In a QCD based model [7, 8] of charmonium production described in section 8, this is justified by arguing that, viewed in the proton rest frame, the $c\bar{c}$ quark pair creation from the photon and the formation of the charmonium state from the $c\bar{c}$ pair both take place over distances considerably greater than the proton radius. The $c\bar{c}$ quark pair is regarded as a colour dipole which interacts with the proton. A prediction of the ratio of the cross-sections for $\psi(2S)$ and J/ψ mesons arising from this model is compared to the measured ratio, presented in section 7.

2 Kinematics

The relevant kinematic quantities are defined in figure 2. For this study, it is demanded that neither the system Y nor the scattered positron e' are observed (see section 4), escaping in the +z (incoming proton) and -z (incoming positron) directions respectively. The system Y is the scattered proton in the elastic case, and otherwise can be considered as the dissociated proton.

The photon-proton centre-of-mass energy, $W_{\gamma p}$, is determined using the relation:

$$W_{\gamma p}^2 \approx \frac{s \sum (E - p_z)}{2E_e} \tag{1}$$

where E_e is the incoming positron energy, and the sum is over the energies, E, and the longitudinal momenta, p_z , of the decay products of the $\psi(2S)$ meson. The centre-of-mass energy of the positron-proton collision is denoted s. Neither the elasticity of the interaction, z, nor the photon virtuality, Q^2 , can be measured. However, the selection criteria restrict the acceptance (see section 5) approximately to the kinematic region z > 0.95, called here quasi-elastic, and $Q^2 < 4 \text{ GeV}^2$; the median Q^2 is expected to be approximately 10^{-4} GeV^2 . Cross-sections are evaluated and presented in the photo-production limit, $Q^2 = 0 \text{ GeV}^2$, in section 6. All cross-sections are integrated over the momentum transfer variable t.

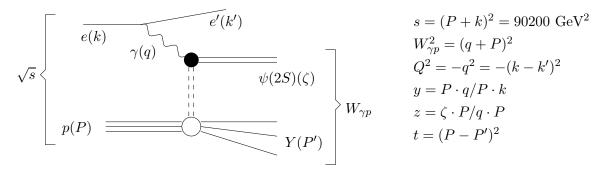


Figure 2: The kinematic variables describing $\psi(2S)$ production at HERA. The incoming positron and proton are denoted e and p respectively, the exchanged photon by γ , the outgoing positron by e', and the $\psi(2S)$ meson produced by $\psi(2S)$. The remainder of the final state is denoted Y. The associated four-momenta are indicated in brackets in the diagram.

3 Experimental Conditions

The data presented here were collected in 1994 and 1995 with the H1 detector at HERA, when 27.5 GeV positrons were in collision with 820 GeV protons. They correspond to an integrated luminosity of 2.7 pb⁻¹ in 1994 and 3.6 pb⁻¹ in 1995.

The H1 detector is described in detail elsewhere [9] and only components relevant to the present analysis are described here. Polar angles are defined with respect to the direction of the incoming proton beam. The Central Tracker (CT) surrounds the interaction region, covering the polar angle range 20° to 165°. Multiwire proportional chambers (CIP and COP) provide additional information for triggering in this region. Forward of the CT is the Forward Tracker (FT) covering the polar angular range 7° to 25°. Surrounding the trackers is a highly segmented liquid argon (LAr) sampling calorimeter [10] consisting of an inner electromagnetic section and an outer hadronic section. Polar angle coverage is from 4° to 153°. During the 1994 data taking a lead scintillator electromagnetic calorimeter (BEMC) covered the angular range 155° to 176° and was able to detect scattered positrons down to a Q^2 of 4 GeV² [11]. This calorimeter was replaced for 1995 data taking by a scintillating fibre and lead calorimeter (SpaCal) with coverage of the angular range 153° to 177.5°, thus extending the acceptance down to a Q^2 of 1.2 GeV² [12]. The tracking chambers are immersed in a uniform axial magnetic field of 1.15 T provided by a superconducting magnet that surrounds the LAr calorimeter. Outside this lies the iron return yoke of the magnet which is instrumented to detect muons in the range 4° to 171°. Luminosity is determined by measuring the rate of the reaction $ep \to ep\gamma$.

A first level trigger accepts events in which a $\psi(2S)$ meson is produced if a track of at least 600 MeV momentum pointing towards an energy cluster greater than about 1 GeV in the LAr calorimeter is identified, or two tracks back-to-back in azimuth in the multiwire proportional chambers (CIP and COP) are found, or if there exists a muon signature in the instrumented iron of the return yoke.

4 Identification of the $\psi(2S)$

The $\psi(2S)$ meson is identified by its decays to $J/\psi(\to e^+e^-)\pi^+\pi^-$, $J/\psi(\to \mu^+\mu^-)\pi^+\pi^-$, e^+e^- and $\mu^+\mu^-$ which have measured branching ratios of 1.95±0.17%, 1.95±0.17%, 0.88±0.13% and 0.77±0.17% respectively [13].

The decay products of the $\psi(2S)$ are measured in the CT and are required to have $p_t > 120 \text{ MeV}$ and $20^{\circ} < \theta < 165^{\circ}$. Particle identification is provided for the leptons by the LAr

calorimeter, in which energy deposits typical for muons or electrons are observed, and for muons by tracks found in the instrumented iron return yoke. It is demanded that the leptons have measured transverse momenta greater than 800 MeV. In the case of the four-particle decays of the $\psi(2S)$, the lepton pair must have a measured effective mass between 2.8 and 3.4 GeV. No particle identification is required for the pions. It is required that no charged particles other than the decay products of the $\psi(2S)$ are observed in the CT or FT. A measured photon-proton centre-of-mass energy, $W_{\gamma p}$, in the range 40-160 (40-120) GeV for the dimuon (dielectron) sample is demanded (see section 5).

Events in which the scattered positron is observed in the backward electromagnetic calorimeter (BEMC in 1994, SpaCal in 1995) or in the LAr calorimeter, are rejected, which restricts the acceptance to the kinematic range $Q^2 < 4$ (1.2) GeV² for the 1994 (1995) data sample. Therefore, in section 6, positron-proton cross-sections are quoted for $Q^2 < 4$ GeV². Events with higher Q^2 are estimated to contribute less than 1% to the sample.

The mass distributions obtained are shown in figures 3(a-d), where the data from 1994 and 1995 and for both di-lepton types are combined. Figure 3(c) shows a clear signal of 27 events with negligible background in the range $M_{\psi(2S)} - M_{J/\psi} - 60 < \Delta M < M_{\psi(2S)} - M_{J/\psi} + 60$ MeV where $\Delta M \equiv M_{(\ell^+\ell^-\pi^+\pi^-)} - M_{(\ell^+\ell^-)}$. The number of events in the $\psi(2S) \to \ell^+\ell^-$ signal is estimated by fitting the mass distribution to two gaussian functions, convoluted with an exponential tail to account for di-electron decays in which one of the decay electrons has lost energy through radiation, above a linear background (figure3(d)). A signal of 50 ± 12 events is obtained. No contribution from $\psi(3770)$ to these signals is expected.

5 Monte Carlo Model and Acceptances

Simulation studies were made to obtain the acceptances and efficiencies of triggering, track reconstruction, selection and lepton identification for the $\psi(2S)$ production processes. These studies used event samples generated with the DIFFVM Monte Carlo generator [14], and a detailed simulation of the H1 detector response based on the GEANT program [15]. DIFFVM generates events according to the cross-section dependence $d\sigma/dt \propto W_{\gamma p}^{4\varepsilon} e^{bt}$ for elastic $\psi(2S)$ production, and $d^2\sigma/dt \, dM_Y^2 \propto W_{\gamma p}^{4\varepsilon} e^{bt} M_Y^{\beta}$ for production with proton dissociation, where M_Y is the effective mass of the hadrons produced in the dissociation of the proton which is related to the elasticity z by $z \approx (W^2 - M_Y^2)/(W^2 - m_p^2)$. The parameters of the DIFFVM generator are chosen such that the features of J/ψ elastic and proton dissociation photo-production processes are reproduced [2, 3]: $4\varepsilon = 0.9$, $b = 4.0 \, \text{GeV}^{-2}$, $b' = 1.6 \, \text{GeV}^{-2}$, $\beta = -2.16$. Equal cross-sections for elastic and proton dissociative photo-production of $\psi(2S)$ are assumed, consistent with the results of the J/ψ analysis. The decay angular distribution for $\psi(2S)$ decaying directly into two leptons is simulated according to s-channel helicity conservation. The Monte Carlo program is found to model all features of the data well, in particular the momentum and angular distributions of the $\psi(2S)$ decay products to which the acceptance is sensitive.

The acceptance is found to be not strongly dependent on $W_{\gamma p}$ in the range $40 < W_{\gamma p} < 120(160)$ GeV for the electron(muon) decay channel. By demanding that the measured value of $W_{\gamma p}$ lies in this region the sensitivity of the measured cross-section to the uncertainty in its $W_{\gamma p}$ dependence is small. The requirement that there be no charged particle observed in the detector, other than the decay products of the $\psi(2S)$ meson, restricts the acceptance approximately to the region z>0.95. Events with z<0.95 are estimated to contribute a background of less than 1% to the signal. Within the kinematic region z>0.95 and $40 < W_{\gamma p} < 120(160)$ GeV the total probability of observing a produced $\psi(2S)$ meson is about 6% for the four-particle decays and 18% for the two-particle decays.

Uncertainties in the acceptance calculations contribute to systematic uncertainties in the cross-section measurements. The uncertainty due to the use of the Monte Carlo model is estimated to be 5% by observing the changes in the acceptance resulting from varying the parameters 4ε by ± 0.1 , b and b' by ± 1.0 GeV⁻², β between -2.00 and -2.50, and by changing the assumed fraction of the quasi-elastic cross-section due to elastically produced $\psi(2S)$ by $\pm 20\%$. Further systematic uncertainties arise due to uncertainties in the precision of the simulation of the H1 detector response. The most significant are 12% due to the track reconstruction efficiency (6% for the two-particle decays), 6% due to the lepton identification efficiency and 6% due to the trigger efficiency. Additionally for the two-particle decays, there is a 20% systematic uncertainty in the cross-section measurement resulting from the choice of the functional form of the fit to the di-lepton mass distribution in figure 3(d). The total systematic uncertainties in the cross-section measurements are 16% for the four-particle decays and 23% for the two-particle decays. Branching ratio (BR) uncertainties of 9% and 18% respectively [13] are given separately below.

6 $\psi(2S)$ Cross-sections

The numbers of events, acceptances, flux factors and cross-sections are given in table 1. For the four-particle decays of the $\psi(2S)$ the results are shown separately for the electron and muon decays, and for the 1994 and 1995 data samples. The corresponding four cross-sections are consistent with one another. A decomposition of the acceptance is given, which shows that, except for the trigger efficiencies, aspects of the acceptance are stable from year to year and decay channel to decay channel. The higher trigger efficiencies in 1994 with respect to 1995 reflect a higher fraction of events in which the trigger fired being recorded for subsequent analysis. This fraction is determined by HERA beam background conditions and global data-taking requirements. For the two-particle decays all data are combined in table 1 because of the lack of statistics of the subsamples in the presence of substantial background.

The combined cross-section from the four-particle decays using 1994 and 1995 data is

$$\sigma\left[e^+p \to e^+\psi(2S)Y\right] = [2.02 \pm 0.39({\rm stat}) \pm 0.33({\rm syst}) \pm 0.18({\rm BR})]$$
nb

for the kinematic range $40 < W_{\gamma p} < 160 \text{ GeV}, Q^2 < 4 \text{ GeV}^2, z > 0.95.$

The photo-production $(Q^2 = 0 \text{ GeV}^2)$ cross-section at $W_{\gamma p} = 80 \text{ GeV}$ is related to the electro-production cross-section by

$$\sigma_{\rm ep} = \sigma_{\gamma p}(W_{\gamma p} = 80 \text{ GeV}) \int dy \int dQ^2 f_{\gamma/e}(y, Q^2) \left(\frac{W_{\gamma p}}{80 \text{ GeV}}\right)^{4\varepsilon} \left(1 + \frac{Q^2}{M_{\psi(2S)}^2}\right)^{-n} \tag{2}$$

where $W_{\gamma p} = m_p^2 - Q^2 + y(s - m_p^2 - m_e^2)$, $4\varepsilon = 0.9$, n = 2. The limits of integration are determined by the kinematic range of the electro-production cross-section. The spectral flux of transverse photons from the electron [16] is

$$f_{\gamma/e}(y,Q^2) = \frac{\alpha}{2 \pi Q^2} \cdot \left[1 + (1-y)^2 - \frac{2m_e^2 y^2}{Q^2} \right].$$
 (3)

Given an approximate $W_{\gamma p}^{0.9}$ dependence of the photo-production cross-section, the choice of $W_{\gamma p}=80$ GeV as the point at which to specify $\sigma_{\gamma p}$ minimises the uncertainty in $\sigma_{\gamma p}$ due to possible deviations from this dependence. Varying the assumed $W_{\gamma p}$ and Q^2 dependences of the virtual photon-proton cross-section in equation 2 (4 ε between 0.8 and 1.0 and n between 1 and 3) results in a systematic uncertainty in the photo-production cross-section of 3%.

For z > 0.95 at $W_{\gamma p} = 80$ GeV, the photoproduction cross-section

$$\sigma [\gamma p \to \psi(2S)Y] = [16.9 \pm 3.3({\rm stat}) \pm 2.7({\rm syst}) \pm 1.5({\rm BR})] \text{ nb}$$

is obtained.

The $\psi(2S)$ signal of 50 ± 12 events from the analysis of the two-particle decay sample yields a statistically independent measurement of the cross-sections for $\psi(2S)$ production:

$$\sigma\left[e^{+}p \to e\psi(2S)Y\right] = [2.65 \pm 0.63({\rm stat}) \pm 0.61({\rm syst}) \pm 0.48({\rm BR})] \ {\rm nb},$$

$$\sigma\left[\gamma p \to \psi(2S)Y\right] = [22.1 \pm 5.3({\rm stat}) \pm 5.1({\rm syst}) \pm 4.0({\rm BR})] \ {\rm nb}$$

for the kinematic intervals above. Here the estimate of the level of background under the $\psi(2S)$ signal contributes a 20% systematic uncertainty.

The results from the samples of two-particle and four-particle decays agree well, so they are combined to give an overall photo-production cross-section of

$$\sigma\left[\gamma p \to \psi(2S)Y\right] = \left[17.9 \pm 2.8 (\mathrm{stat}) \pm 2.7 (\mathrm{syst}) \pm 1.4 (\mathrm{BR})\right] \text{ nb}$$

at $W_{\gamma p} = 80 \text{ GeV}$, for z > 0.95.

7 The Cross-section Ratio $\sigma\left[\psi(2S)\right]/\sigma\left[J/\psi\right]$

The J/ψ quasi-elastic (z > 0.95) photo-production cross-section at $W_{\gamma p} = 80$ GeV is (119.5 \pm 11.2 \pm 12.0) nb [3], yielding a ratio:

$$\frac{\sigma\left[\gamma p \to \psi(2S)Y\right]}{\sigma\left[\gamma p \to J/\psi Y\right]} = 0.150 \pm 0.027(\mathrm{stat}) \pm 0.018(\mathrm{syst}) \pm 0.011(\mathrm{BR}).$$

Figure 4 contains a compilation of measurements from fixed target experiments of the ratio of the photon-nucleon cross-sections for the production of $\psi(2S)$ and J/ψ mesons: three photoproduction experiments at $Q^2=0~{\rm GeV}^2$ (deuterium target [17] SLAC, lithium target [18] NA14, and deuterium target [19] E401) plus muo-production experiments on an iron target [20](EMC) and more recently on tin and carbon [21](NMC). Of these the deuterium target data samples were restricted to events in which the decay products of the vector mesons were the only tracks detected; in the lithium and iron target data some contribution from the kinematic region of lower z was included. Despite the different experimental conditions, it is apparent that in going from fixed target to HERA energies there is no significant change in the $\psi(2S)$ to J/ψ cross-section ratio.

8 Colour Dipole Calculation

By considering the $c\bar{c}$ quark pair as a colour dipole of transverse size r, cross-sections for the photo-production of charmonium can be calculated in the framework of QCD [7, 8]. The amplitude of forward photo-production on the proton can be written

$$\int d^2 \vec{r} \ \Psi_V(\vec{r})^* \sigma(\vec{r}) \Psi_\gamma(\vec{r}) \tag{4}$$

where $\Psi_{\gamma}(\vec{r})$ is the wave-function representing the probability of finding a $c\bar{c}$ dipole of size $r = |\vec{r}|$ in the photon, $\sigma(\vec{r})$ is the colour dipole cross-section, and $\Psi_{V}(\vec{r})$ the transverse wave-function of the charmonium state. The product $\sigma(\vec{r})\Psi_{\gamma}(\vec{r})$ is calculated in QCD using the approximation of

a two-gluon exchange between the colour dipole and the proton. It is found that, approximately, $\Psi_{\gamma}(\vec{r}) \propto \exp(-m_c r)$ and $\sigma(\vec{r}) \sim r^2$, so that the product is a function peaking at $r \approx 2/m_c$. As a result the matrix element, and hence the cross-section, is sensitive to the radial wave-function of the charmonium around $r = 2/m_c$. This feature influences the ratio of the cross-sections for the production of $\psi(2S)$ and $J/\psi(1S)$ mesons. There is a relative suppression of the $\psi(2S)$ because its wave-function has a radial node (the value of r for which $\Psi_V(\vec{r}) = 0$) near to $r = 2/m_c$, in contrast to the J/ψ wave-function. Therefore the ratio of these cross-sections provides a test of the model which is free of many normalisation uncertainties.

A prediction for the ratio of the forward elastic photo-production cross-sections of 0.17 is obtained [8], which agrees well with the ratio of quasi-elastic cross-sections reported here. This agreement supports the hypothesis that the charmonium production cross-section is sensitive to the radial wave-function of the meson away from the origin, resulting in a suppression of the production of the 2S state, $\psi(2S)$, with respect to the 1S state, J/ψ .

9 Summary

Measurements of the quasi-elastic photo-production cross-section for $\psi(2S)$ at a $W_{\gamma p}$ value of 80 GeV at HERA have been reported. The ratio between the quasi-elastic $\psi(2S)$ and J/ψ photo-production cross-sections is compatible with those measured at lower energies. A prediction from a QCD based model in which the photon fluctuates into a $c\bar{c}$ quark pair which then behaves as a colour dipole in its interaction with the proton is in good agreement with the measured ratio.

Acknowledgments

We are grateful to the HERA machine group whose outstanding efforts have made and continue to make this experiment possible. We thank the engineers and technicians for their work in constructing and maintaining the H1 detector, our funding agencies for financial support, the DESY technical staff for continual assistance, and the DESY directorate for the hospitality which they extend to the non–DESY members of the collaboration.

References

- [1] T. Ahmed et al., H1 Collaboration Phys. Lett. B338 (1994) 507
- [2] S. Aid *et al.*, H1 Collaboration *Nucl. Phys.* B468 (1996) 3
- [3] S. Aid et al., H1 Collaboration Nucl. Phys. B472 (1996) 3
- [4] M. Derrick et al., Zeus Collaboration Phys. Lett. B350 (1995) 120
- [5] J. Breitweg et al., Zeus Collaboration Z. Phys. C75 (1997) 215
- [6] M. Derrick et al., Zeus Collaboration, DESY-97-147 (1997)
- [7] B.Z. Kopeliovich and B.G. Zakharov, Phys. Rev. D44 (1991) 3466
- [8] B.Z. Kopeliovich, J. Nemchik, N.N. Nikolaev and G.G. Zakharov, Phys. Lett. B309 (1993) 179
- [9] The H1 Detector at HERA, I. Abt et al., H1 Collaboration, Nucl. Inst. Meth. A386 (1997) 310, 348

- [10] B. Andrieu et al., H1 Calorimeter Group, Nucl. Inst. Meth. A336 (1993) 460
- [11] J. Ban et al., H1 BEMC Group Nucl. Inst. Meth. A372 (1996) 399
- [12] T.Nicholls et al., Nucl. Inst. Meth. A374 (1996) 149;
 R.D. Appuhn et al., Nucl. Inst. Meth. A386 (1997) 397
- [13] R. Barnett et al., Particle Data Group, Phys. Rev. D54 (1996) 1
- [14] B. List Diploma Thesis Techn. Univ. Berlin (1993) unpublished
- [15] R. Brun et al., CERN-DD/EE-84-1 (1987)
- [16] V. M. Budnev et al., Phys. Rep. C 15 (1975) 181;
 C.F.Weizsäcker, Z. Phys. 88 (1934) 612;
 E.J.Williams, Phys. Rev. 45 (1934) 729
- [17] U. Camerini et al., Phys. Rev. Lett. 35 (1975) 483
- [18] R. Barate et al., NA14 Collab., Z. Phys. C33 (1987) 505
- [19] M. Binkley et al., E401 Collab., Phys. Rev. Lett. 50 (1983) 302
- [20] J.J. Aubert et al., EMC Collab., Nucl. Phys. B213 (1983) 1
- [21] P. Amaudraz et al., NMC Collab., Nucl. Phys. B371 (1992) 553

Data	$e^{+}e^{-}\pi^{+}\pi^{-}$	$e^{+}e^{-}\pi^{+}\pi^{-}$	
sample	(1994)	(1995)	
$W_{\gamma p} \; (\text{GeV})$	40 - 120	40 - 120	
$Q^2 (\text{GeV}^2)$	$Q^2 < 4.0$	$Q^2 < 1.2$	
Luminosity (pb^{-1})	2.70	3.59	
Angular acceptance	0.495	0.492	
p_t track acceptance	0.715	0.704	
Trigger efficiency	0.431	0.195	
Analysis efficiency	0.514	0.514	
Total acceptance	0.078	0.035	
Signal events	5	4	
$\sigma(ep o e\psi(2S)Y)/{ m nb}$	$1.21 \pm .54 \pm .20$	$1.64 \pm .82 \pm .33$	
$\Phi_{\gamma/e}$	0.088	0.085	
$\sigma(\gamma p o \psi(2S)Y)/\mathrm{nb}$	$13.7 \pm 6.1 \pm 2.3$	$19.3 \pm 9.6 \pm 3.9$	

Data	$\mu^{+}\mu^{-}\pi^{+}\pi^{-}$	$\mu^{+}\mu^{-}\pi^{+}\pi^{-}$	$\ell^+\ell^-(\ell=\mu,e)$
sample	(1994)	(1995)	(1994+1995)
$W_{\gamma p} \; (\text{GeV})$	40 - 160	40 - 160	40 - 160
$Q^2 (\text{GeV}^2)$	$Q^2 < 4.0$	$Q^2 < 1.2$	$Q^2 < 4.0$
Luminosity (pb^{-1})	2.72	3.63	6.37
Angular acceptance	0.628	0.622	0.614
p_t track acceptance	0.715	0.712	0.994
Trigger efficiency	0.367	0.207	0.487
Analysis efficiency	0.518	0.606	0.588
Total acceptance	0.085	0.055	0.178
Signal events	10	8	49.6
$\sigma(ep o e\psi(2S)Y)/{ m nb}$	$2.21\pm.70\pm.37$	$2.06 \pm .73 \pm .39$	$2.65 \pm .63 \pm .61$
$\Phi_{\gamma/e}$	0.120	0.115	0.120
$\sigma(\gamma p o \psi(2S)Y)/{ m nb}$	$18.5 \pm 5.8 \pm 3.1$	$17.9 \pm 6.3 \pm 3.4$	$22.1 \pm 5.3 \pm 5.1$

Table 1: Summary of signals, acceptances, and the quasi-elastic (z > 0.95) electro- and photo-production cross-sections for the five data samples. The first error shown is statistical and the second systematic. Uncertainties due to the imprecisely known branching ratios of the $\psi(2S)$ decays are not included. The ranges over $W_{\gamma p}$ and Q^2 over which the ep cross section measurement is made are shown. Angular and p_t track acceptance refer to the fraction of events in the kinematic range in which all decay products fall within the angular and p_t ranges of acceptance, respectively. Trigger efficiency indicates the probability that such an event is accepted by the first level trigger, and the analysis efficiency gives the probability of subsequently meeting all further selection criteria (see section 4). $\Phi_{\gamma/e}$ is the photon flux factor used to give photo-production cross-sections at a fixed $W_{\gamma p}$ of 80 GeV.

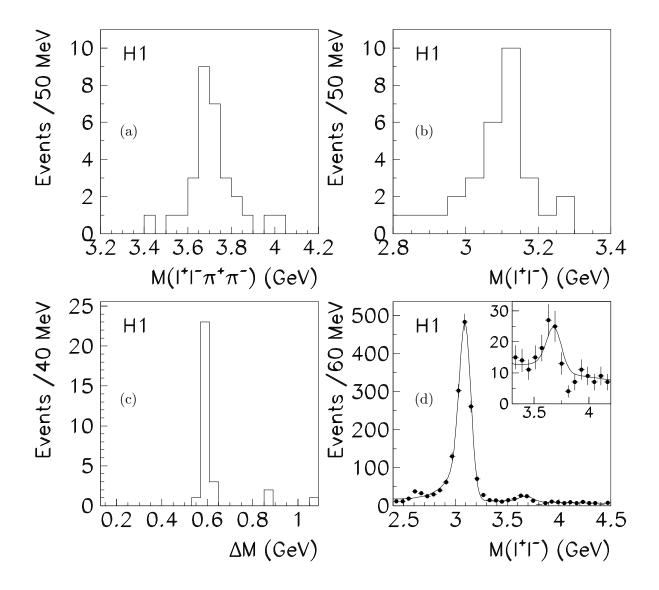


Figure 3: The effective mass plots for the four track sample: (a) the four track effective mass, (b) the di-lepton effective mass, and (c) the ΔM distribution where $\Delta M = M_{(l^+l^-\pi^+\pi^-)} - M_{(l^+l^-)}$. (d) Effective mass distributions for the two track sample: the di-lepton effective mass with a fit to two gaussians, convoluted with an exponential tail to account for di-electron decays in which a decay electron has lost energy through radiation before entering the detector, plus a linear background.

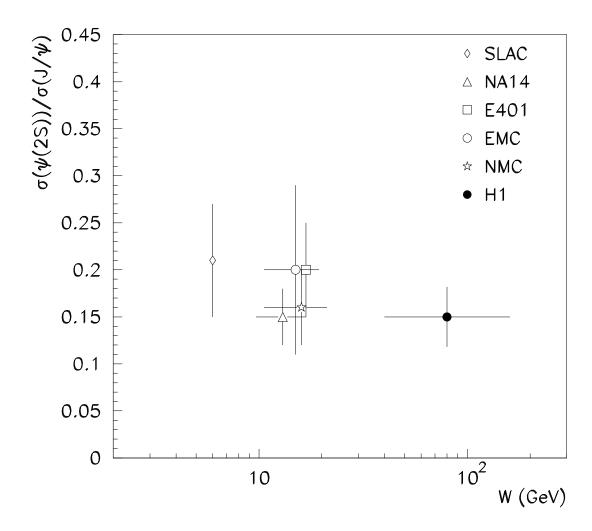


Figure 4: The ratio of the cross-sections for $\psi(2S)$ and J/ψ photo-production on nucleons as a function of photon-proton centre-of-mass energy, $W_{\gamma p}$. The results from the present analysis are shown together with those from earlier fixed target experiments [17, 18, 19, 20, 21]. The ratios from the fixed target experiments have been corrected using the latest decay branching ratios. The error bars shown on the low energy measurements are statistical only. The combined statistical and systematic errors are shown for the H1 result. Horizontal bars indicate the ranges of $W_{\gamma p}$ over which the measurements were made, where they are specified. The common uncertainty due to the imprecisely known branching ratios is not shown.